Measurement of $e^+e^- \to pK^-\bar{\Lambda} + c.c.$ cross sections between 4.009 GeV and 4.951 GeV

BESIII

The BESIII collaboration

E-mail: besiii-publications@ihep.ac.cn

ABSTRACT: Using e^+e^- collision datasets corresponding to a total integrated luminosity of $21.7\,\mathrm{fb}^{-1}$ collected with the BESIII detector at the BEPCII collider at center-of-mass energies ranging from $4.009\,\mathrm{GeV}$ to $4.951\,\mathrm{GeV}$, the energy-dependent cross sections of $e^+e^- \to pK^-\bar{\Lambda} + c.c.$ are measured for the first time. By fitting these energy-dependent cross sections, we search for the excited ψ states $\psi(4160)$ and $\psi(4415)$, and the vector charmonium-like states $\psi(4230)$, $\psi(4360)$, and $\psi(4660)$. No evidence for these is observed and the upper limits on the branching fractions of these states decaying into $pK^-\bar{\Lambda} + c.c.$ are set at the 90% confidence level.

Contents

1 Introduction

In the last two decades, a large number of charmonium-like vector states ψ have been discovered [1] in the hidden or open charm final states. The $\psi(4260)$ was first observed by the BaBar Collaboration in the process of $e^+e^- \to \gamma_{\mathrm{ISR}}\pi^+\pi^- J/\psi$ [2], where ISR denotes initial state radiation. The $\psi(4360)$ and $\psi(4660)$ were found by the Belle and BaBar Collaborations in the $\pi^+\pi^-\psi(2S)$ final states [3, 4]. Later, a precise study on the process $e^+e^- \to \pi^+\pi^- J/\psi$ by the BESIII Collaboration revealed two structures with masses of $4222.0 \pm 3.1 \pm 1.4\,\mathrm{MeV}/c^2$ and $4320.0 \pm 10.4 \pm 7.0\,\mathrm{MeV}/c^2$ in the $\psi(4260)$ region [5]. The former one, renamed as $Y(4230)$ [1], was further confirmed by the BESIII Collaboration in the decay channels $e^+e^- \to \omega\chi_{c0}$ [6], $e^+e^- \to \pi^+\pi^- h_c$ [7], $e^+e^- \to \pi^+ D^0 D^{*-}$ [8], $e^+e^- \to \eta J/\psi$ [9], $e^+e^- \to \pi^+\pi^+\psi(3686)$ [10], and $e^+e^- \to \pi^+ D^{*0} D^{*-}$ [11]. Since some properties of these states cannot be explained by the conventional charmonium model, they are usually regarded as candidates for the exotic states, such as hybrids, tetraquarks, and molecules [12–14].

On the other side, although several processes with light hadron final states, such as $e^+e^- \to p\bar{p}\pi^0$ [15], $e^+e^- \to p\bar{p}\eta(\omega)$ [16], $e^+e^- \to p\bar{n}K_S^0 K^-$ [17], $e^+e^- \to K_S^0 K^\pm \pi^\mp \pi^0(\eta)$ [18], $e^+e^- \to \omega\pi^+\pi^-$ [19], have been studied, no significant charmonium-like states were found in these until now. A further broad search for the potential exotic structures in more light hadron final states is highly desirable.

In this analysis, the cross sections of the process $e^+e^- \to pK^-\bar{\Lambda} + c.c.$ are measured by analyzing $21.7\,\mathrm{fb}^{-1}$ of e^+e^- collision data taken at center-of-mass energies $(\sqrt{s})$ ranging from $4.009\,\mathrm{GeV}$ to $4.951\,\mathrm{GeV}$. The vector charmonium(-like) states, $\psi(4160)$, $\psi(4230)$, $\psi(4360)$, $\psi(4415)$, and $\psi(4660)$ are investigated by fitting the obtained energy-dependent cross sections. Throughout the paper, the charged-conjugation mode is always implied, unless explicitly stated.

2 Detector and data sets

The BESIII detector is a magnetic spectrometer [20] located at the Beijing Electron Positron Collider (BEPCII) [21]. The cylindrical core of the BESIII detector consists of a main drift chamber filled with helium-based gas (MDC), a plastic scintillator time-of-flight system (TOF), and a CsI(Tl) electromagnetic calorimeter (EMC), which are all enclosed in a superconducting solenoidal magnet providing a 1.0 T magnetic field. The flux-return yoke is instrumented with resistive plate chambers arranged in 9 layers in the barrel and 8 layers in the endcaps for muon identification. The acceptance of charged particles and photons is 93% of 4π solid angle. The charged-particle momentum resolution at $1.0\,\mathrm{GeV}/c$ is 0.5%, and the specific energy loss resolution is 6% for the electrons from Bhabha scattering. The EMC measures photon energies with a resolution of 2.5% (5%) at $1\,\mathrm{GeV}$ in the barrel (end cap) region. The time resolution of the TOF barrel part is 68 ps, while that of the end cap part is 110 ps. The end cap TOF system was upgraded in 2015 with multi-gap resistive plate chamber technology, providing a time resolution of 60 ps [22–24]. All of those are enclosed in a superconducting solenoidal magnet providing a 1.0 T magnetic field [25].

The data samples used in this analysis were collected by the BESIII detector at 37 energy points between $4.009\,\mathrm{GeV}$ and $4.951\,\mathrm{GeV}$. The center-of-mass energies and the corresponding integrated luminosities [26, 27] at various energy points are shown in table 1. Simulated samples produced with the GEANT4-based [28] Monte-Carlo (MC) software, which includes the geometric description of the BESIII detector and the detector response, are used to determine the detection efficiencies and to estimate the background levels. The simulation includes the beam energy spread and ISR in the e^+e^- annihilations modeled with the generator KKMC [29]. The inclusive MC simulation samples generated at $\sqrt{s} = 4.178\,\mathrm{GeV}$ with 40 times the luminosity of the data sample are used to analyze the possible background contributions. They consist of open charm production processes, ISR production of vector charmonium or charmonium-like states, and continuum processes $(e^+e^- \to q\bar{q}, q = u, d, s)$. The open charm production processes are generated using CONEXC [30], and the ISR production is incorporated in KKMC [29]. The known decay states are modeled with BESEVENTGEN [31, 32] using branching fractions taken from the Particle Data Group (PDG) [1] and the remaining unknown decays from the charmonium states are modeled with LUNDCHARM [33, 34]. The final state radiation from charged final state particles is incorporated with the PHOTOS [35] package. The signal MC samples of $e^+e^- \to pK^-\bar{\Lambda}$ are generated by using the amplitude model with parameters fixed to the amplitude analysis results [36].

3 Event selection and background analysis

To select the candidates for $e^+e^- \to pK^-\bar{\Lambda}$, the Λ is reconstructed with the charged decay mode, and hence there are only four charged tracks $p\bar{p}\pi^\pm K^\mp$ in the final states. All charged tracks are required to satisfy $|d_z| < 20$ cm and $|\cos\theta| < 0.93$. Here, $|d_z|$ is the coordinate of the charged particle production point along the beam axis and θ is the polar angle of the charged track. For each event, four charged tracks with zero net charge are required. Since

$\sqrt{s}$ (GeV)	$\mathcal{L}_{\mathrm{int}}$ (pb^{-1})	N_{sig}	ϵ (%)	$(1+\delta)$	$\frac{1}{1-\Pi^2}$	σ^{B} (pb)
4.009	482.0±4.7	754 ± 28	20.2	1.16	1.04	10.1 ± 0.4 ± 0.4
4.129	401.5±2.6	507 ± 24	20.1	1.19	1.05	7.9 ± 0.4 ± 0.3
4.157	408.7±2.6	463 ± 23	20.4	1.20	1.05	6.9 ± 0.3 ± 0.3
4.178	3189.0±31.9	4025 ± 67	20.3	1.20	1.05	7.7 ± 0.1 ± 0.3
4.189	526.7±2.2	658 ± 27	20.3	1.21	1.06	7.6 ± 0.3 ± 0.4
4.199	526.0±2.5	639 ± 26	20.4	1.21	1.06	7.3 ± 0.3 ± 0.3
4.209	517.1±1.8	618 ± 25	20.1	1.21	1.06	7.3 ± 0.3 ± 0.3
4.219	514.6±1.8	639 ± 27	19.4	1.22	1.06	7.8 ± 0.3 ± 0.3
4.226	1100.9±7.0	1247 ± 38	20.4	1.22	1.06	6.8 ± 0.2 ± 0.3
4.236	530.3±2.4	630 ± 26	19.8	1.22	1.06	7.3 ± 0.3 ± 0.3
4.244	538.1±2.7	570 ± 25	20.3	1.23	1.06	6.3 ± 0.3 ± 0.5
4.258	828.4±5.5	932 ± 32	20.5	1.23	1.05	6.6 ± 0.2 ± 0.7
4.267	531.1±3.1	589 ± 25	20.4	1.23	1.05	6.6 ± 0.3 ± 0.5
4.278	175.7±1.0	197 ± 15	20.1	1.24	1.05	6.7 ± 0.5 ± 0.6
4.288	502.4±3.3	496 ± 24	19.8	1.24	1.05	6.0 ± 0.3 ± 0.4
4.312	501.2±3.3	566 ± 23	19.8	1.25	1.05	6.8 ± 0.3 ± 0.4
4.337	505.0±3.4	520 ± 24	20.1	1.26	1.05	6.1 ± 0.3 ± 0.3
4.358	543.9±3.6	550 ± 25	21.0	1.26	1.05	5.7 ± 0.3 ± 0.3
4.377	522.7±3.5	529 ± 24	20.3	1.27	1.05	5.9 ± 0.3 ± 0.3
4.397	507.8±3.4	449 ± 23	20.3	1.27	1.05	5.1 ± 0.3 ± 0.2
4.416	1090.7±7.2	1030 ± 33	20.4	1.28	1.05	5.4 ± 0.2 ± 0.2
4.436	569.9±3.8	523 ± 24	20.2	1.29	1.05	5.3 ± 0.2 ± 0.3
4.467	111.1±0.8	90 ± 10	20.2	1.30	1.05	4.6 ± 0.5 ± 0.3
4.527	112.1±0.8	87 ± 9	19.8	1.32	1.05	4.4 ± 0.5 ± 0.2
4.600	586.9±4.0	416 ± 21	21.8	1.35	1.05	3.6 ± 0.2 ± 0.2
4.612	103.7±0.6	81 ± 9	21.1	1.36	1.05	4.0 ± 0.5 ± 0.3
4.628	521.5±2.8	357 ± 20	20.7	1.38	1.05	3.6 ± 0.2 ± 0.2
4.641	551.7±3.0	375 ± 20	20.7	1.37	1.05	3.6 ± 0.2 ± 0.2
4.661	529.4±2.8	351 ± 20	20.7	1.38	1.05	3.5 ± 0.2 ± 0.2
4.682	1667.4±8.9	1012 ± 34	20.6	1.39	1.05	3.2 ± 0.1 ± 0.2
4.699	535.5±2.9	362 ± 20	20.2	1.39	1.05	3.6 ± 0.2 ± 0.2
4.740	163.9±0.9	115 ± 11	20.9	1.40	1.05	3.5 ± 0.3 ± 0.3
4.750	366.6±2.0	248 ± 17	20.8	1.41	1.05	3.4 ± 0.2 ± 0.2
4.781	511.5±2.7	288 ± 19	20.5	1.42	1.06	2.9 ± 0.2 ± 0.2
4.843	525.1±2.8	235 ± 17	20.0	1.47	1.06	2.3 ± 0.2 ± 0.2
4.918	207.8±1.1	127 ± 11	19.1	1.55	1.06	3.1 ± 0.3 ± 0.2
4.951	159.3±0.9	63 ± 9	18.5	1.59	1.06	2.0 ± 0.3 ± 0.2

Table 1. The Born cross sections of the $e^+e^- \to pK^-\bar{\Lambda} + c.c.$ process at various energy points. Here $\mathcal{L}_{\mathrm{int}}$ is the integrated luminosity, N_{sig} is the number of signal events from the fit to the $M_{p\pi^-}$ distribution, ϵ is the detection efficiency, $(1+\delta)$ is the radiative correction factor including vacuum polarization effect, $\frac{1}{1-\Pi^2}$ is the vacuum polarization factor, and σ^{B} is the Born cross section. The first uncertainties are statistical and the second are systematic.

the background from particle mis-identification is negligible and the particle identification detectors are not optimized in the momentum region above $1\,\mathrm{GeV}$, we don't apply any particle identification.

To reconstruct the candidates for Λ, all possible opposite charged track pairs will be assigned as $p\pi^-$. The $p\pi^-$ trajectories are constrained to originate from a common vertex by applying a vertex fit, and the χ^2 of the vertex fit is required to be less than 100. The Λ candidate is constrained in a secondary vertex fit to originate from the interaction point. The decay length of the Λ candidate must be greater than twice the vertex resolution. The invariant mass of the $p\pi^-$ combination is required to be within $1.10 < M_{p\pi^-} < 1.13\,\mathrm{GeV}/c^2$ to suppress wrong assignments. Exactly one Λ candidate per event is required to satisfy the selection criteria. The other two charged tracks are assigned according to their charges as proton and kaon not from Λ decays. To ensure that the two charged tracks originate from the interaction point, they are imposed with additional requirements of $|d_z| < 10$ cm and $|d_r| < 1$ cm. Here, $|d_r|$ is the distance between the charged track production point and the beam axis in the plane perpendicular to the beam axis.

To further suppress background and improve track momentum resolution, a four-momentum constraint (4C) kinematic fit is imposed on the initial e^+e^- beam energy under the hypothesis of $e^+e^- \to pK^-\bar{\Lambda}$. The χ^2 of the kinematic fit is required to be less than 100. To reduce the number of background events caused by spurious kaons originating from Bhabha scattering events interacting with the materials in the detector, the events with $|\cos\theta_K| > 0.83$ are vetoed, where θ_K is the polar angle of the charged kaon.

After applying all of the above selection criteria, studies of the inclusive MC sample indicate that the total background fraction is only 1.8%. The background contributions are categorized into the peaking background, such as $e^+e^- \to \pi^+\Lambda\bar{\Sigma}^-$, and non-peaking background, such as $e^+e^- \to \rho^0 p\bar{p}$. Given that the peaking background fraction is lower than 1.0%, it is neglected in the further analysis and will be considered as one source of systematic uncertainties.

4 Cross section measurement

To obtain the $e^+e^- \to pK^-\bar{\Lambda}$ signal yield, an un-binned maximum likelihood fit is performed to the invariant mass spectrum of $M_{p\pi^-}$. The signal is described with the MC-determined shape convolved with a Gaussian function to consider the difference between data and MC simulation. The background shape is parametrized as a linear function. As an example, figure 1 shows the fit result of the accepted candidates in data at $\sqrt{s} = 4.178\,\mathrm{GeV}$, and all the signal yields (N_{sig}) at 37 energy points are listed in table 1.

The reconstruction efficiencies are determined with the signal MC samples generated based on the amplitude analysis results in ref. [36]. For the energy points without amplitude fit due to limited statistics, their signal MC samples are generated based on the result of nearby energy point. Figure 2 shows the distributions of polar angles and momenta of final state particles, as well as the invariant mass spectra of all two-particle combinations of signal candidates in data and MC simulation at $\sqrt{s} = 4.178\,\mathrm{GeV}$.
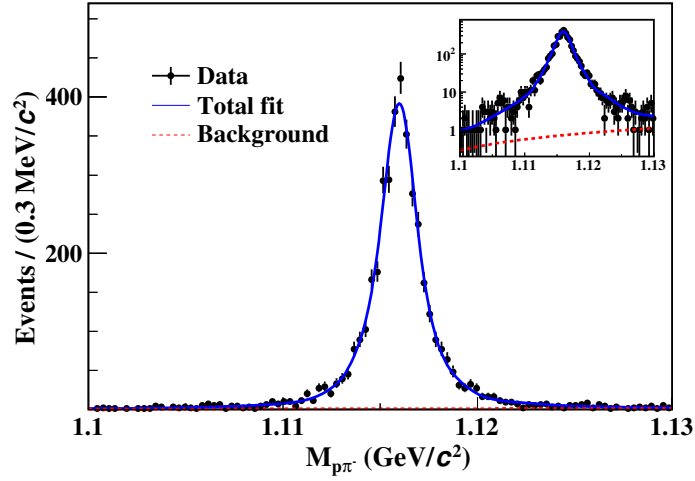
Figure 1. Fit result to the $p\pi^-$ invariant mass distribution of $e^+e^- \to pK^-\bar{\Lambda} + c.c.$. The points with errors are data at $\sqrt{s} = 4.178\,\mathrm{GeV}$, the blue curve is the fit result, and the red dashed curve is the background contribution.
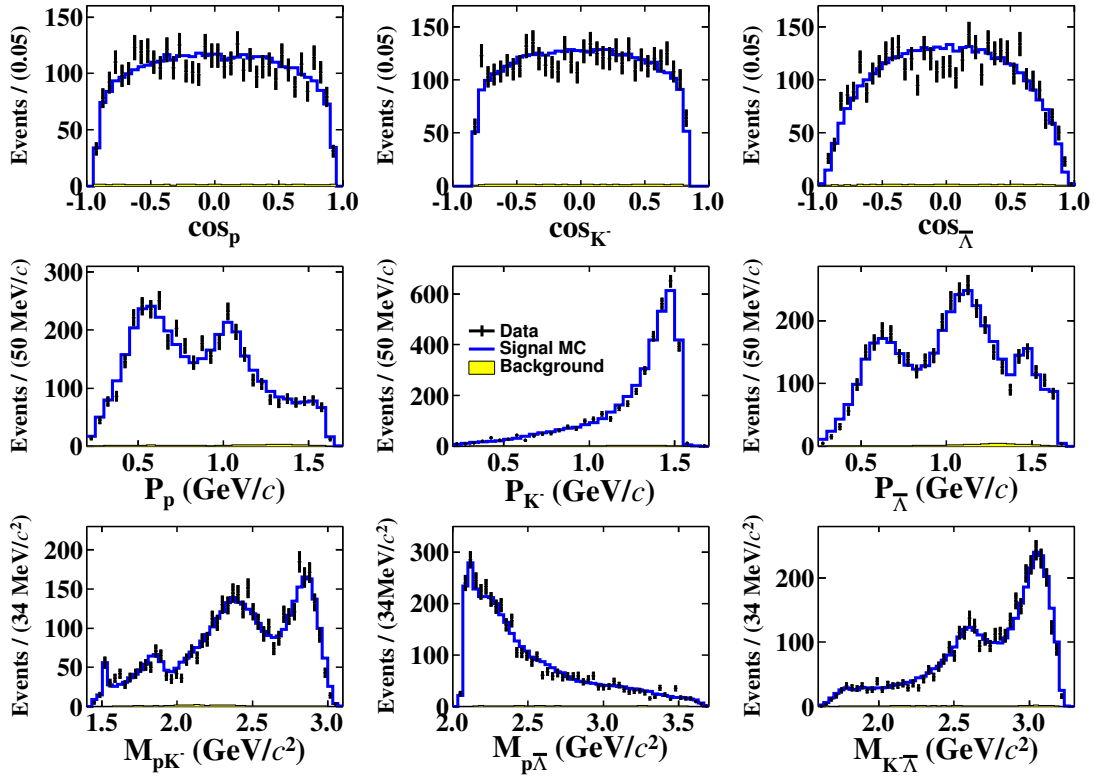

Figure 2. Distributions of $\cos\theta$, the momenta of daughter particles, and the invariant masses of all two-particle combinations at $\sqrt{s} = 4.178\,\mathrm{GeV}$. The points with error bars are data, the blue solid curves are signal MC events, and the yellow hatched histogram is the normalized simulated background.

The Born cross section at a given center-of-mass energy is calculated as

$$\sigma^{\mathrm{B}} = \frac{N_{\mathrm{sig}}}{\mathcal{L}_{\mathrm{int}} \times \mathcal{B} \times \epsilon(1+\delta)\frac{1}{|1-\Pi|^2}}, \tag{4.1}$$

where N_{sig} is the fitted signal yield, $\mathcal{L}_{\mathrm{int}}$ is the integrated luminosity, $\mathcal{B}$ is the branching fraction of the Λ charged decay [1], ϵ is the detection efficiency, $(1+\delta)$ is the ISR correction factor, and $\frac{1}{|1-\Pi|^2}$ is the vacuum polarization factor [30].

To obtain the ISR correction factor, an iterative procedure is performed. First, a series of signal MC samples are generated for all energy points with a constant cross section. The cross sections are calculated based on the reconstruction efficiencies and correction factors obtained from the signal MC simulation. The line shape $\mathcal{P}^4(1 - e^{-\Delta M/p_0})$ is used to describe the measured cross sections, where $\mathcal{P}^4$ is a forth-order polynomial with free parameters, p_0 is a free parameter, and $\Delta M = \sqrt{s} - 2.645\,\mathrm{GeV}$ since no signal event is observed with the data sample at $\sqrt{s} = 2.645\,\mathrm{GeV}$, which is close to the mass threshold of $pK^-\bar{\Lambda}$. Then, the method introduced in ref. [37] is used to get the ISR correction factors and efficiencies, and a new series of cross sections is obtained. This procedure is repeated until the difference of $(1+\delta)\epsilon$ between two subsequent iterations is less than 0.1%. The vacuum polarization factor $\frac{1}{|1-\Pi|^2}$ is obtained from CONEXC [30]. Table 1 summarizes the Born cross sections together with the relevant values used to determine them. The energy-dependent dressed cross sections of $e^+e^- \to pK^-\bar{\Lambda}$, defined as $\sigma^{\mathrm{D}} = \sigma^{\mathrm{B}} \times \frac{1}{|1-\Pi|^2}$, are shown in figure 3.

5 Systematic uncertainty

The systematic uncertainties on the cross section measurement include several sources, as summarized in table 2. They are estimated as described below.

The integrated luminosity is measured using Bhabha scattering events, with an uncertainty less than 1.0% [26, 27]. The uncertainty related to the tracking efficiency of kaons is estimated to be 1.0% using a control sample of $e^+e^- \to K^+K^-\pi^+\pi^-$ and that of protons not from Λ is estimated to be 2.0% using a control sample of $e^+e^- \to p\pi^-\bar{p}\pi^+$. The total systematic uncertainty from tracking is assigned as a linear sum of kaon and non-Λ proton contributions. The systematic uncertainty due to the Λ reconstruction efficiency including tracking efficiencies of the $p\pi^-$ pair, decay length requirement, mass window, vertex fit, and second vertex fit, is assigned as 2.0% using the control sample of $J/\psi(\psi(3686)) \to \Lambda\bar{\Lambda}$ [38]. The systematic uncertainty related to the $N_{\mathrm{trk}} = 4$ requirement, i.e. the number of charged tracks must be four, is estimated to be 0.5% with a control sample of $J/\psi \to pK^-\bar{\Lambda}$ following ref. [39].

The systematic uncertainty of the MC modeling is estimated with a new signal MC sample, in which all fitted complex coupling constants, quoted resonance parameters are smeared with their uncertainties. The difference between the detection efficiencies obtained with the new signal MC sample and the nominal one is taken as this uncertainty. The systematic uncertainty from the fit to the $M_{p\pi^-}$ spectrum is taken into account in two aspects. The uncertainty associated with the fit range is estimated by varying the fit range by 1 MeV. The uncertainty from the background shape is estimated by using a second-order

$\sqrt{s}$ (GeV)	Lum	Trk	Λ Rec	N_{trk}	MC	Fit	KMfit	$\cos\theta$	$1+\delta$	pBKG	BF	Total
4.009	1.0	3.0	2.0	0.5	0.7	0.8	0.3	0.7	0.5	1.0	0.8	4.2
4.129	1.0	3.0	2.0	0.5	1.0	0.4	0.3	0.3	0.5	1.0	0.8	4.2
4.157	1.0	3.0	2.0	0.5	0.9	0.4	0.5	0.5	0.5	1.0	0.8	4.2
4.178	1.0	3.0	2.0	0.5	1.6	0.4	0.3	0.4	0.5	1.0	0.8	4.4
4.189	1.0	3.0	2.0	0.5	1.3	2.0	0.4	0.2	0.5	1.0	0.8	4.7
4.199	1.0	3.0	2.0	0.5	0.7	0.3	0.4	0.3	0.5	1.0	0.8	4.1
4.209	1.0	3.0	2.0	0.5	0.3	0.6	0.3	0.4	0.5	1.0	0.8	4.1
4.219	1.0	3.0	2.0	0.5	1.2	1.5	0.4	0.3	0.5	1.0	0.8	4.5
4.226	1.0	3.0	2.0	0.5	1.7	1.8	0.2	0.5	0.5	1.0	0.8	4.7
4.236	1.0	3.0	2.0	0.5	0.3	1.0	0.4	0.4	0.5	1.0	0.8	4.2
4.244	1.0	3.0	2.0	0.5	5.7	1.5	0.5	0.1	0.5	1.0	0.8	7.2
4.258	1.0	3.0	2.0	0.5	9.6	0.7	0.3	0.4	0.5	1.0	0.8	10.5
4.267	1.0	3.0	2.0	0.5	7.1	0.6	0.4	0.7	0.5	1.0	0.8	8.2
4.278	1.0	3.0	2.0	0.5	6.8	2.6	0.2	0.4	0.5	1.0	0.8	8.3
4.288	1.0	3.0	2.0	0.5	5.5	1.2	0.3	0.7	0.5	1.0	0.8	7.0
4.312	1.0	3.0	2.0	0.5	5.1	0.2	0.3	0.5	0.5	1.0	0.8	6.5
4.337	1.0	3.0	2.0	0.5	3.4	0.7	0.3	0.1	0.5	1.0	0.8	5.4
4.358	1.0	3.0	2.0	0.5	1.1	3.0	0.4	0.5	0.5	1.0	0.8	5.2
4.377	1.0	3.0	2.0	0.5	2.3	0.4	0.3	0.2	0.5	1.0	0.8	4.6
4.397	1.0	3.0	2.0	0.5	2.4	0.3	0.3	1.0	0.5	1.0	0.8	4.8
4.416	1.0	3.0	2.0	0.5	0.2	0.6	0.3	0.2	0.5	1.0	0.8	4.1
4.436	1.0	3.0	2.0	0.5	2.9	1.2	0.3	0.7	0.5	1.0	0.8	5.1
4.467	1.0	3.0	2.0	0.5	0.9	4.0	0.4	0.8	0.5	1.0	0.8	5.8
4.527	1.0	3.0	2.0	0.5	1.1	1.1	0.4	0.9	0.5	1.0	0.8	4.4
4.600	1.0	3.0	2.0	0.5	3.1	0.3	0.3	0.8	0.6	1.0	0.8	5.2
4.612	1.0	3.0	2.0	0.5	4.6	1.2	0.3	1.1	0.8	1.0	0.8	6.4
4.628	1.0	3.0	2.0	0.5	2.4	0.6	0.6	0.6	1.4	1.0	0.8	5.0
4.641	1.0	3.0	2.0	0.5	1.3	0.4	0.4	0.3	0.8	1.0	0.8	4.3
4.661	1.0	3.0	2.0	0.5	3.9	1.0	0.3	0.4	0.8	1.0	0.8	5.8
4.682	1.0	3.0	2.0	0.5	5.1	1.0	0.4	0.5	1.0	1.0	0.8	6.6
4.699	1.0	3.0	2.0	0.5	3.1	1.1	0.4	0.3	0.7	1.0	0.8	5.2
4.740	1.0	3.0	2.0	0.5	6.2	1.2	0.7	0.9	1.0	1.0	0.8	7.6
4.750	1.0	3.0	2.0	0.5	4.2	1.5	0.3	0.5	1.1	1.0	0.8	6.1
4.781	1.0	3.0	2.0	0.5	3.6	2.2	0.4	0.1	1.5	1.0	0.8	6.0
4.843	1.0	3.0	2.0	0.5	5.2	1.3	0.4	3.8	1.3	1.0	0.8	7.8
4.918	1.0	3.0	2.0	0.5	6.3	0.0	0.4	1.6	1.9	1.0	0.8	7.9
4.951	1.0	3.0	2.0	0.5	4.4	3.5	0.4	0.8	3.3	1.0	0.8	7.7

Table 2. The relative systematic uncertainties (in %) on the cross section measurement, which include luminosity (Lum), tracking efficiency (Trk), Λ reconstruction efficiency (Λ Rec), MC modeling (MC), fit to $M_{p\pi^-}$ (Fit), 4C kinematic fit (KMfit), $|\cos\theta_K| < 0.83$ ($\cos\theta$), correction factor $(1+\delta)$, Λ peaking background (pBKG), and $\mathcal{B}(\Lambda \to p\pi^-)$ branching fraction (BF).

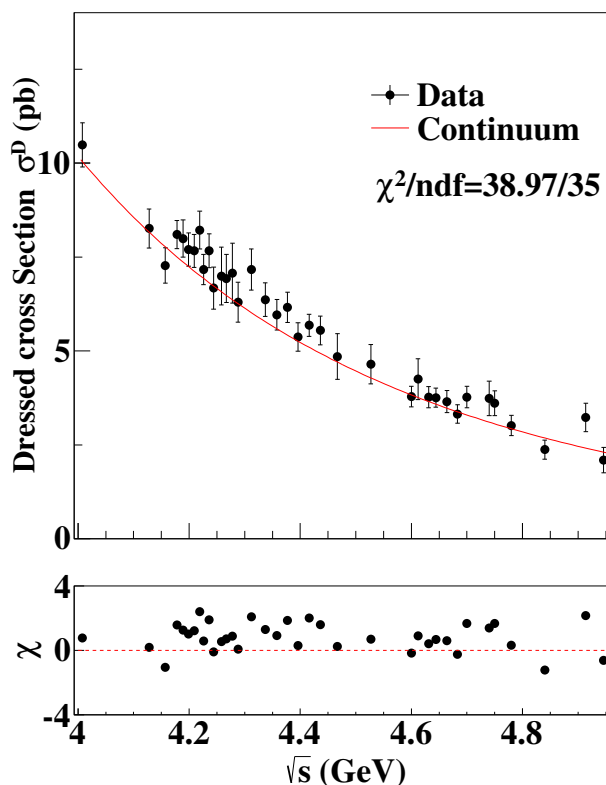**Figure 3**. The energy-dependent dressed cross sections of the process $e^+e^- \to pK^-\bar{\Lambda} + c.c.$. The points with error bars are the measured values including both statistical and systematic uncertainties. The red solid curve is the fit result only with the continuum contribution a/s^n. Due to the correlated systematic uncertainties, most of the χ values are positive by minimizing eq. (6.1).

polynomial function. For each of these two aspects, the maximum difference between the signal yields obtained with nominal and alternative background shapes is taken as the corresponding systematic uncertainty. Adding these two items in quadrature, we obtain the relevant systematic uncertainty.

The systematic uncertainty related to the 4C kinematic fit is estimated by comparing the detection efficiencies with and without the helix parameter correction [40], taking the difference as the corresponding systematic uncertainty. The systematic uncertainty of the $|\cos\theta_K| < 0.83$ requirement is estimated by varying the cut range by 0.01. The maximum difference between the cross sections obtained with nominal and alternative cut ranges is taken to be the corresponding systematic uncertainty. The systematic uncertainty related to the correction factor is considered in two aspects. The uncertainty due to the theoretical uncertainty of the vacuum polarization factor is assigned to be 0.5% [30]. The uncertainty due to the line shape used in the iteration is estimated by varying all free parameters of the line shape within their statistical uncertainties. The distribution of σ^B obtained with the alternative parameter sets is fitted with a Gaussian function (μ_1, σ_1). The uncertainty is assigned to be $(|\mu_1 - \mu_0| + \sigma_1)/\mu_0 \times 100\%$, where μ_0 is the nominal value. Adding these two items in quadrature gives the systematic uncertainty in the correction factor. The

systematic uncertainty due to the Λ peaking background is assigned as 1.0% since the fraction of this background from the inclusive MC sample is found to be less than 1.0%. The systematic uncertainty of the quoted branching fraction of $\Lambda \to p\pi^-$ is 0.8%.

6 Fit to the cross sections of $e^+e^- \to pK^-\bar{\Lambda} + c.c.$

In order to search for possible charmless decays of charmonium(-like) states $\psi \to pK^-\bar{\Lambda}+c.c.$, we try two kinds of least chi-square fits to the dressed cross sections. The χ^2 is constructed as

$$\chi^2 = (\Delta\vec{\sigma})^T V^{-1} \Delta\vec{\sigma}, \tag{6.1}$$

where $\Delta\vec{\sigma}_i = \sigma_i - \sigma_i^{\text{fit}}(\vec{\theta})$ and V is the covariance matrix. The σ_i and σ_i^{fit} are the measured and fitted values for the cross section at the i-th energy point, respectively. The covariance matrix is constructed as $V_{ii} = V_{\text{sta},i} + V_{\text{sys},i}$ for diagonal elements and $V_{ij} = \sqrt{V_{\text{corr-sys},i} \times V_{\text{corr-sys},j}}$ for off-diagonal elements ($i \neq j$). Here, $V_{\text{corr-sys}}$ includes the systematic uncertainties of integrated luminosity, tracking, Λ reconstruction, and $\mathcal{B}(\Lambda \to p\pi^-)$.

In the first fit, the cross sections are assumed to result only from continuum production and to follow a relation of a/s^n. The fit result is shown in figure 3, with the goodness-of-fit of $\chi^2/\text{ndf} = 39.05/35$, where both statistical and systematic uncertainties are included and ndf denotes the number of degrees of freedom. In the second fit, the cross section is modeled as a coherent sum of continuum production and resonant amplitudes, e.g., $\sigma(\sqrt{s}) = |a/s^n + BW(\sqrt{s})e^{i\phi}|^2$, where

$$BW\left(\sqrt{s}\right) = \frac{M}{\sqrt{s}} \frac{\sqrt{12\pi\Gamma_{\text{ee}}\Gamma_{\text{tot}}\mathcal{B}(\mathcal{R} \to pK^-\bar{\Lambda} + c.c.)}}{s - M^2 + iM\Gamma_{\text{tot}}} \sqrt{\frac{PS\left(\sqrt{s}\right)}{PS(M)}} \tag{6.2}$$

is used to describe charmonium-(like) states. Here, M, Γ_{tot}, and Γ_{ee} are the mass, full width, and e^+e^- partial width of the resonance $\mathcal{R}$, respectively. $\mathcal{B}(\mathcal{R} \to pK^-\bar{\Lambda} + c.c.)$ denotes the branching fraction of the decay $\mathcal{R} \to pK^-\bar{\Lambda} + c.c.$, ϕ is the relative phase between the continuum and resonance, and $\frac{PS(\sqrt{s})}{PS(M)}$ is the three-body phase space factor. In the second case, the values of M and Γ_{tot} are fixed to the PDG values [1]. As shown in figure 4, several well established charmonium-(like) states, $\psi(4160), \psi(4230), \psi(4360), \psi(4415)$, and $\psi(4660)$, are checked and no evidence for any $\psi(Y) \to pK^-\bar{\Lambda} + c.c.$ decay is found. To set the upper limits of $\Gamma_{\text{ee}}\mathcal{B}(\mathcal{R} \to pK^-\bar{\Lambda} + c.c.)$, the likelihood distributions are constructed as $L(\Gamma_{\text{ee}}\mathcal{B}) = e^{-0.5\chi^2}$. The upper limits at the 90% confidence level (C.L.) is obtained by integrating $L(\Gamma_{\text{ee}}\mathcal{B})$ from zero to 90% of the total curve. The uncertainty associated with the quoted resonance parameters of $\mathcal{R}$ is studied by sampling its parameters according to its uncertainty, repeating the estimation of upper limits, and taking the width of resulting distribution as this uncertainty. The upper limit is assigned as the nominal value plus the uncertainty due to quoted resonance parameters, as summarized in table 3

7 Summary

In summary, with the $21.7\,\text{fb}^{-1}$ of e^+e^- collision data taken at $\sqrt{s}$ ranging from $4.009\,\text{GeV}$ to $4.951\,\text{GeV}$, the energy-dependent cross sections of $e^+e^- \to pK^-\bar{\Lambda}$ are measured for the

Resonance	$M_{\mathcal{R}}$ (MeV/c^2)	$\Gamma_{\mathcal{R}}$ (MeV)	$\Gamma_{ee}\mathcal{B}(\mathcal{R} \to pK^-\bar{\Lambda} + c.c.)$ (eV)
$\psi(4160)$	4191 ± 5	70 ± 10	$< 3.0 \times 10^{-3}$
$\psi(4230)$	4223 ± 3	48 ± 8	$< 1.3 \times 10^{-3}$
$\psi(4360)$	4374 ± 4	118 ± 12	$< 4.7 \times 10^{-3}$
$\psi(4415)$	4421 ± 4	62 ± 20	$< 3.4 \times 10^{-3}$
$\psi(4660)$	4630 ± 6	72 ± 14	$< 2.8 \times 10^{-3}$

Table 3. Fixed masses ($M_{\mathcal{R}}$) and widths ($\Gamma_{\mathcal{R}}$) together with the upper limits on the product of the e^+e^- partial width and branching fraction of $\mathcal{R} \to pK^-\bar{\Lambda} + c.c.$, $\Gamma_{ee}\mathcal{B}(\mathcal{R} \to pK^-\bar{\Lambda} + c.c.)$ at the 90% C.L. for different charmonium(-like) state.
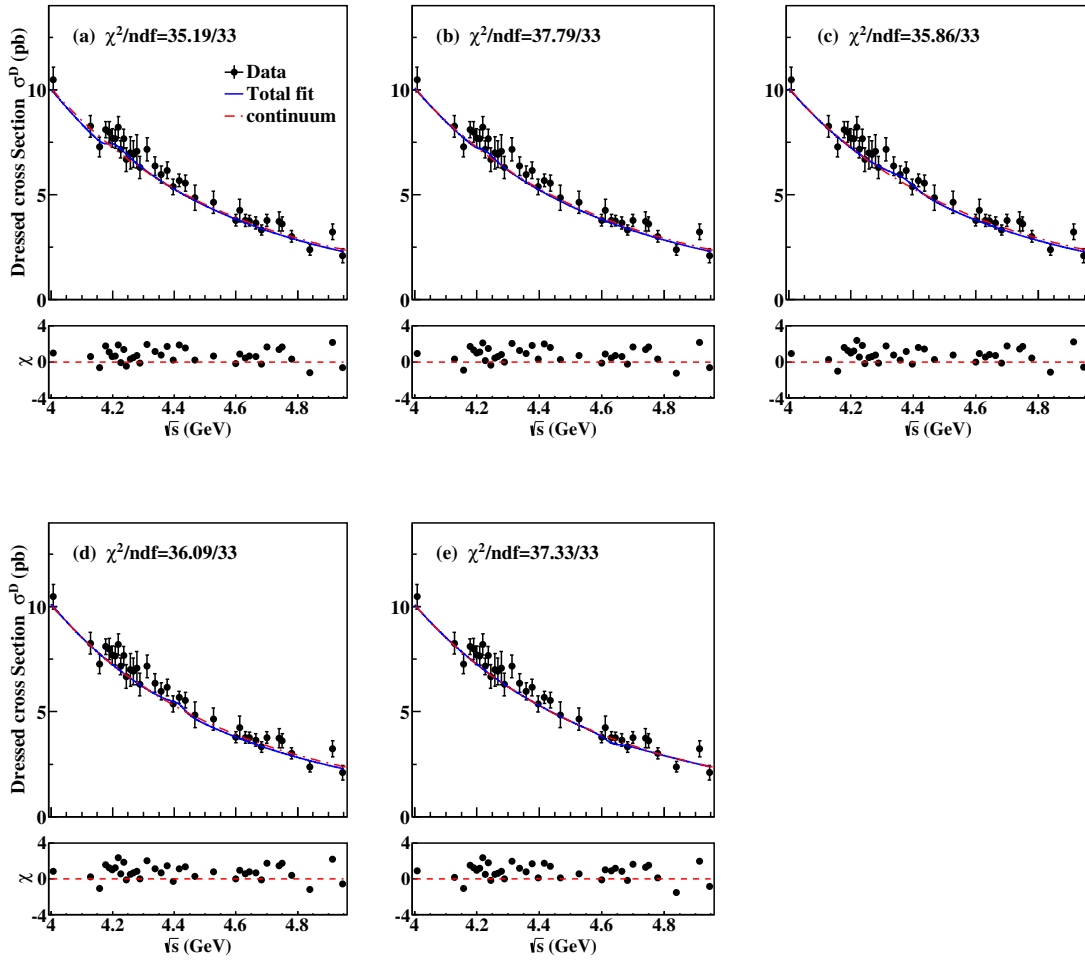
Figure 4. Fits to the energy-dependent dressed cross sections of $e^+e^- \to pK^-\bar{\Lambda} + c.c.$ under the hypotheses of continuum production plus (a) $\psi(4160)$, (b) $\psi(4230)$, (c) $\psi(4360)$, (d) $\psi(4415)$, and (e) $\psi(4660)$. The points with error bars are the measured values including both statistical and systematic uncertainties. The blue solid curve is the total fit result and the red dash curve is the continuum contribution a/s^n.

first time. We fit the obtained cross sections under different hypotheses of charmonium(-like) states plus continuum production. No evidence for any decay of charmonium(-like) states is found and the upper limits of $\Gamma_{ee}\mathcal{B}(\mathcal{R} \to pK^-\bar{\Lambda} + c.c.)$ at the 90% C.L. are given.

References

[1] Particle Data Group collaboration, *Review of Particle Physics*, *PTEP* **2022** (2022) 083C01 [INSPIRE].

[2] BaBar collaboration, *Observation of a broad structure in the $\pi^+\pi^- J/\psi$ mass spectrum around 4.26-GeV/c^2*, *Phys. Rev. Lett.* **95** (2005) 142001 [hep-ex/0506081] [INSPIRE].

[3] Belle collaboration, *Observation of two resonant structures in $e^+e^- \to \pi^+\pi^-\psi(2s)$ via initial-state radiation at belle*, *Phys. Rev. Lett.* **99** (2007) 142002 [arXiv:0707.3699] [INSPIRE].

[4] BaBar collaboration, *Evidence of a broad structure at an invariant mass of 4.32 GeV/c² in the reaction $e^+e^- \to \pi^+\pi^-\psi(2S)$ measured at BaBar*, *Phys. Rev. Lett.* **98** (2007) 212001 [hep-ex/0610057] [INSPIRE].

[5] BESIII collaboration, *Precise Measurement of the $e^+e^- \to \pi^+\pi^- J/\psi$ Cross Section at Center-of-Mass Energies from 3.77 to 4.60 GeV*, *Phys. Rev. Lett.* **118** (2017) 092001 [arXiv:1611.01317] [INSPIRE].

[6] BESIII collaboration, *Study of $e^+e^- \to \omega\chi_{cJ}$ at Center of Mass Energies from 4.21 to 4.42 GeV*, *Phys. Rev. Lett.* **114** (2015) 092003 [arXiv:1410.6538] [INSPIRE].

[7] BESIII collaboration, *Evidence of Two Resonant Structures in $e^+e^- \to \pi^+\pi^- h_c$*, *Phys. Rev. Lett.* **118** (2017) 092002 [arXiv:1610.07044] [INSPIRE].

[8] BESIII collaboration, *Evidence of a Resonant Structure in the $e^+e^- \to \pi^+ D^0 D^{*-}$ Cross Section between 4.05 and 4.60 GeV*, *Phys. Rev. Lett.* **122** (2019) 102002 [arXiv:1808.02847] [INSPIRE].

[9] BESIII collaboration, *Observation of the $y(4220)$ and $y(4390)$ in the process $e^+e^- \to \eta j/\psi$*, *Phys. Rev. D* **102** (2020) 031101 [arXiv:2003.03705] [INSPIRE].

[10] BESIII collaboration, *Cross section measurement of $e^+e^- \to \pi^+\pi^-\psi(3686)$ from $\sqrt{s} = 4.0076$ GeV to 4.6984 gev*, *Phys. Rev. D* **104** (2021) 052012 [arXiv:2107.09210] [INSPIRE].

[11] BESIII collaboration, *Observation of three charmoniumlike states with $J^{PC} = 1^{--}$ in $e^+e^- \to D^{*0}D^{*-}\pi^+$*, *Phys. Rev. Lett.* **130** (2023) 121901 [arXiv:2301.07321] [INSPIRE].

[12] N. Brambilla et al., *Heavy quarkonium: progress, puzzles, and opportunities*, *Eur. Phys. J. C* **71** (2011) 1534 [arXiv:1010.5827] [INSPIRE].

[13] H.-X. Chen, W. Chen, X. Liu and S.-L. Zhu, *The hidden-charm pentaquark and tetraquark states*, *Phys. Rept.* **639** (2016) 1 [arXiv:1601.02092] [INSPIRE].

[14] Y.-R. Liu et al., *Pentaquark and tetraquark states*, *Prog. Part. Nucl. Phys.* **107** (2019) 237 [arXiv:1903.11976] [INSPIRE].

[15] BESIII collaboration, *Measurements of cross section of $e^+e^- \to p\bar{p}\pi^0$ at center-of-mass energies between 4.008 and 4.600 GeV*, *Phys. Lett. B* **771** (2017) 45 [arXiv:1701.04198] [INSPIRE].

[16] BESIII collaboration, *Cross section measurement of $e^+e^- \to p\bar{p}\eta$ and $e^+e^- \to p\bar{p}\omega$ at center-of-mass energies between 3.773 GeV and 4.6 GeV*, *Phys. Rev. D* **104** (2021) 092008 [arXiv:2102.04268] [INSPIRE].

[17] BESIII collaboration, *First measurement of $e^+e^- \to pK_S^0\bar{n}K^- + c.c.$ above open charm threshold*, *Phys. Rev. D* **98** (2018) 032014 [arXiv:1807.03468] [INSPIRE].

[18] BESIII collaboration, *Measurements of $e^+e^- \to K_S^0 K^\pm \pi^\mp \pi^0$ and $K_S^0 K^\pm \pi^\pm \eta$ at center-of-mass energies from 3.90 to 4.60 GeV*, *Phys. Rev. D* **99** (2019) 012003 [arXiv:1810.09395] [INSPIRE].

[19] BESIII collaboration, *Study of the $e^+e^- \to \pi^+\pi^-\omega$ process at center-of-mass energies between 4.0 and 4.6 GeV*, *JHEP* **08** (2023) 159 [arXiv:2303.09718] [INSPIRE].

[20] BESIII collaboration, *Design and construction of the BESIII detector*, *Nucl. Instrum. Meth. A* **614** (2010) 345 [arXiv:0911.4960] [INSPIRE].

[21] C. Yu et al., *BEPCII Performance and Beam Dynamics Studies on Luminosity*, in the proceedings of the *7th International Particle Accelerator Conference*, Busan, Korea, Republic of, May 08–13 (2016), p. TUYA01 [DOI:10.18429/JACoW-IPAC2016-TUYA01] [INSPIRE].

[22] X. Li et al., *Study of MRPC technology for BESIII endcap-TOF upgrade*, *Radiat. Detect. Technol. Methods* **1** (2017) 13.

[23] Y.X. Guo *et al.*, *The study of time calibration for upgraded end cap TOF of BESIII*, *Radiat. Detect. Technol. Methods* **1** (2017) 15.

[24] P. Cao et al., *Design and construction of the new BESIII endcap Time-of-Flight system with MRPC Technology*, *Nucl. Instrum. Meth. A* **953** (2020) 163053 [INSPIRE].

[25] K.-X. Huang et al., *Method for detector description transformation to Unity and application in BESIII*, *Nucl. Sci. Tech.* **33** (2022) 142 [arXiv:2206.10117] [INSPIRE].

[26] BESIII collaboration, *Precision measurement of the integrated luminosity of the data taken by BESIII at center-of-mass energies between 3.810 GeV and 4.600 GeV*, *Chin. Phys. C* **39** (2015) 093001 [arXiv:1503.03408] [INSPIRE].

[27] BESIII collaboration, *Luminosities and energies of e^+e^- collision data taken between 4.61 gev and 4.95 GeV at BESIII*, *Chin. Phys. C* **46** (2022) 113003 [arXiv:2205.04809] [INSPIRE].

[28] GEANT4 collaboration, *GEANT4 — a simulation toolkit*, *Nucl. Instrum. Meth. A* **506** (2003) 250 [INSPIRE].

[29] S. Jadach, B.F.L. Ward and Z. Was, *Coherent exclusive exponentiation for precision Monte Carlo calculations*, *Phys. Rev. D* **63** (2001) 113009 [hep-ph/0006359] [INSPIRE].

[30] R.-G. Ping, *An exclusive event generator for e^+e^- scan experiments*, *Chin. Phys. C* **38** (2014) 083001 [arXiv:1309.3932] [INSPIRE].

[31] D.J. Lange, *The EvtGen particle decay simulation package*, *Nucl. Instrum. Meth. A* **462** (2001) 152 [INSPIRE].

[32] R.-G. Ping, *Event generators at BESIII*, *Chin. Phys. C* **32** (2008) 599 [INSPIRE].

[33] J.C. Chen et al., *Event generator for J/ψ and $\psi(2S)$ decay*, *Phys. Rev. D* **62** (2000) 034003 [INSPIRE].

[34] R.-L. Yang, R.-G. Ping and H. Chen, *Tuning and validation of the Lundcharm model with J/ψ decays*, *Chin. Phys. Lett.* **31** (2014) 061301 [INSPIRE].

[35] E. Richter-Was, *QED bremsstrahlung in semileptonic B and leptonic τ decays*, *Phys. Lett. B* **303** (1993) 163 [INSPIRE].

[36] BESIII collaboration, *Determination of Spin-parity Quantum Numbers for the Narrow Structure Near the $p\bar{\Lambda}$ Threshold in $e^+e^- \to pK^-\bar{\Lambda} + c.c.$*, *Phys. Rev. Lett.* **131** (2023) 151901 [arXiv:2303.01989] [INSPIRE].

[37] W. Sun et al., *An iterative weighting method to apply ISR correction to e^+e^- hadronic cross-section measurements*, *Front. Phys. (Beijing)* **16** (2021) 64501 [arXiv:2011.07889] [INSPIRE].

[38] BESIII collaboration, *Study of J/ψ and $\psi(3686)$ decay to $\Lambda\overline{\Lambda}$ and $\Sigma^0\overline{\Sigma}^0$ final states*, *Phys. Rev. D* **95** (2017) 052003 [arXiv:1701.07191] [INSPIRE].

[39] BESIII collaboration, *First measurement of the absolute branching fraction of $\Lambda \to p\mu^-\overline{\nu}_\mu$*, *Phys. Rev. Lett.* **127** (2021) 121802 [arXiv:2107.06704] [INSPIRE].

[40] BESIII collaboration, *Search for hadronic transition $\chi_{cJ} \to \eta_c\pi^+\pi^-$ and observation of $\chi_{cJ} \to K\overline{K}\pi\pi$*, *Phys. Rev. D* **87** (2013) 012002 [arXiv:1208.4805] [INSPIRE].

The BESIII collaboration

M. Ablikim[1], M.N. Achasov[13,b], P. Adlarson[75], X.C. Ai[81], R. Aliberti[36], A. Amoroso[74A,74C], M.R. An[40], Q. An[71,58], Y. Bai[57], O. Bakina[37], I. Balossino[30A], Y. Ban[47,g], V. Batozskaya[1,45], K. Begzsuren[33], N. Berger[36], M. Berlowski[45], M. Bertani[29A], D. Bettoni[30A], F. Bianchi[74A,74C], E. Bianco[74A,74C], J. Bloms[68], A. Bortone[74A,74C], I. Boyko[37], R.A. Briere[5], A. Brueggemann[68], H. Cai[76], X. Cai[1,58], A. Calcaterra[29A], G.F. Cao[1,63], N. Cao[1,63], S.A. Cetin[62A], J.F. Chang[1,58], T.T. Chang[77], W.L. Chang[1,63], G.R. Che[44], G. Chelkov[37,a], C. Chen[44], Chao Chen[55], G. Chen[1], H.S. Chen[1,63], M.L. Chen[1,58,63], S.J. Chen[43], S.M. Chen[61], T. Chen[1,63], X.R. Chen[32,63], X.T. Chen[1,63], Y.B. Chen[1,58], Y.Q. Chen[35], Z.J. Chen[26,h], W.S. Cheng[74C], S.K. Choi[10], X. Chu[44], G. Cibinetto[30A], S.C. Coen[4], F. Cossio[74C], J.J. Cui[50], H.L. Dai[1,58], J.P. Dai[79], A. Dbeyssi[19], R. E. de Boer[4], D. Dedovich[37], Z.Y. Deng[1], A. Denig[36], I. Denysenko[37], M. Destefanis[74A,74C], F. De Mori[74A,74C], B. Ding[66,1], X.X. Ding[47,g], Y. Ding[41], Y. Ding[35], J. Dong[1,58], L.Y. Dong[1,63], M.Y. Dong[1,58,63], X. Dong[76], S.X. Du[81], Z.H. Duan[43], P. Egorov[37,a], Y.L. Fan[76], J. Fang[1,58], S.S. Fang[1,63], W.X. Fang[1], Y. Fang[1], R. Farinelli[30A], L. Fava[74B,74C], F. Feldbauer[4], G. Felici[29A], C.Q. Feng[71,58], J.H. Feng[59], K Fischer[69], M. Fritsch[4], C. Fritzsch[68], C.D. Fu[1], J.L. Fu[63], Y.W. Fu[1], H. Gao[63], Y.N. Gao[47,g], Yang Gao[71,58], S. Garbolino[74C], I. Garzia[30A,30B], P.T. Ge[76], Z.W. Ge[43], C. Geng[59], E.M. Gersabeck[67], A Gilman[69], K. Goetzen[14], L. Gong[41], W.X. Gong[1,58], W. Gradl[36], S. Gramigna[30A,30B], M. Greco[74A,74C], M.H. Gu[1,58], Y.T. Gu[16], C. Y Guan[1,63], Z.L. Guan[23], A.Q. Guo[32,63], L.B. Guo[42], M.J. Guo[50], R.P. Guo[49], Y.P. Guo[12,f], A. Guskov[37,a], T.T. Han[50], W.Y. Han[40], X.Q. Hao[20], F.A. Harris[65], K.K. He[55], K.L. He[1,63], F.H. Heinsius[4], C.H. Heinz[36], Y.K. Heng[1,58,63], C. Herold[60], T. Holtmann[4], P.C. Hong[12,f], G.Y. Hou[1,63], X.T. Hou[1,63], Y.R. Hou[63], Z.L. Hou[1], H.M. Hu[1,63], J.F. Hu[56,i], T. Hu[1,58,63], Y. Hu[1], G.S. Huang[71,58], K.X. Huang[59], L.Q. Huang[32,63], X.T. Huang[50], Y.P. Huang[1], T. Hussain[73], N Hüsken[28,36], W. Imoehl[28], M. Irshad[71,58], J. Jackson[28], S. Jaeger[4], S. Janchiv[33], J.H. Jeong[10], Q. Ji[1], Q.P. Ji[20], X.B. Ji[1,63], X.L. Ji[1,58], Y.Y. Ji[50], X.Q. Jia[50], Z.K. Jia[71,58], P.C. Jiang[47,g], S.S. Jiang[40], T.J. Jiang[17], X.S. Jiang[1,58,63], Y. Jiang[63], J.B. Jiao[50], Z. Jiao[24], S. Jin[43], Y. Jin[66], M.Q. Jing[1,63], T. Johansson[75], X. Kui[1], S. Kabana[34], N. Kalantar-Nayestanaki[64], X.L. Kang[9], X.S. Kang[41], R. Kappert[64], M. Kavatsyuk[64], B.C. Ke[81], A. Khoukaz[68], R. Kiuchi[1], R. Kliemt[14], O.B. Kolcu[62A], B. Kopf[4], M.K. Kuessner[4], A. Kupsc[45,75], W. Kühn[38], J.J. Lane[67], P. Larin[19], A. Lavania[27], L. Lavezzi[74A,74C], T.T. Lei[71,k], Z.H. Lei[71,58], H. Leithoff[36], M. Lellmann[36], T. Lenz[36], C. Li[48], C. Li[44], C.H. Li[40], Cheng Li[71,58], D.M. Li[81], F. Li[1,58], G. Li[1], H. Li[71,58], H.B. Li[1,63], H.J. Li[20], H.N. Li[56,i], Hui Li[44], J.R. Li[61], J.S. Li[59], J.W. Li[50], K.L. Li[20], Ke Li[1], L. J Li[1,63], L.K. Li[1], Lei Li[3], M.H. Li[44], P.R. Li[39,j,k], Q.X. Li[50], S.X. Li[12], T. Li[50], W.D. Li[1,63], W.G. Li[1], X.H. Li[71,58], X.L. Li[50], Xiaoyu Li[1,63], Y.G. Li[47,g], Z.J. Li[59], Z.X. Li[16], C. Liang[43], H. Liang[71,58], H. Liang[35], H. Liang[1,63], Y.F. Liang[54], Y.T. Liang[32,63], G.R. Liao[15], L.Z. Liao[50], J. Libby[27], A. Limphirat[60], D.X. Lin[32,63], T. Lin[1], B.J. Liu[1], B.X. Liu[76], C. Liu[35], C.X. Liu[1], D. Liu[19,71], F.H. Liu[53], Fang Liu[1], Feng Liu[6], G.M. Liu[56,i], H. Liu[39,j,k], H.B. Liu[16], H.M. Liu[1,63], Huanhuan Liu[1], Huihui Liu[22], J.B. Liu[71,58], J.L. Liu[72], J.Y. Liu[1,63], K. Liu[1], K.Y. Liu[41], Ke Liu[23], L. Liu[71,58], L.C. Liu[44], Lu Liu[44], M.H. Liu[12,f], P.L. Liu[1], Q. Liu[63], S.B. Liu[71,58], T. Liu[12,f], W.K. Liu[44], W.M. Liu[71,58], X. Liu[39,j,k], Y. Liu[39,j,k], Y. Liu[81], Y.B. Liu[44], Z.A. Liu[1,58,63], Z.Q. Liu[50], X.C. Lou[1,58,63], F.X. Lu[59], H.J. Lu[24], J.G. Lu[1,58], X.L. Lu[1], Y. Lu[7], Y.P. Lu[1,58], Z.H. Lu[1,63], C.L. Luo[42], M.X. Luo[80], T. Luo[12,f], X.L. Luo[1,58], X.R. Lyu[63], Y.F. Lyu[44], F.C. Ma[41], H.L. Ma[1],

J.L. Ma[1,63], L.L. Ma[50], M.M. Ma[1,63], Q.M. Ma[1], R.Q. Ma[1,63], R.T. Ma[63], X.Y. Ma[1,58], Y. Ma[47,g], Y.M. Ma[32], F.E. Maas[19], M. Maggiora[74A,74C], S. Malde[69], A. Mangoni[29B], Y.J. Mao[47,g], Z.P. Mao[1], S. Marcello[74A,74C], Z.X. Meng[66], J.G. Messchendorp[14,64], G. Mezzadri[30A], H. Miao[1,63], T.J. Min[43], R.E. Mitchell[28], X.H. Mo[1,58,63], N. Yu. Muchnoi[13,b], Y. Nefedov[37], F. Nerling[19,d], I.B. Nikolaev[13,b], Z. Ning[1,58], S. Nisar[11,l], Y. Niu [50], S.L. Olsen[63], Q. Ouyang[1,58,63], S. Pacetti[29B,29C], X. Pan[55], Y. Pan[57], A. Pathak[35], P. Patteri[29A], Y.P. Pei[71,58], M. Pelizaeus[4], H.P. Peng[71,58], K. Peters[14,d], J.L. Ping[42], R.G. Ping[1,63], S. Plura[36], S. Pogodin[37], V. Prasad[34], F.Z. Qi[1], H. Qi[71,58], H.R. Qi[61], M. Qi[43], T.Y. Qi[12,f], S. Qian[1,58], W.B. Qian[63], C.F. Qiao[63], J.J. Qin[72], L.Q. Qin[15], X.P. Qin[12,f], X.S. Qin[50], Z.H. Qin[1,58], J.F. Qiu[1], S.Q. Qu[61], C.F. Redmer[36], K.J. Ren[40], A. Rivetti[74C], V. Rodin[64], M. Rolo[74C], G. Rong[1,63], Ch. Rosner[19], S.N. Ruan[44], N. Salone[45], A. Sarantsev[37,c], Y. Schelhaas[36], K. Schoenning[75], M. Scodeggio[30A,30B], K.Y. Shan[12,f], W. Shan[25], X.Y. Shan[71,58], J.F. Shangguan[55], L.G. Shao[1,63], M. Shao[71,58], C.P. Shen[12,f], H.F. Shen[1,63], W.H. Shen[63], X.Y. Shen[1,63], B.A. Shi[63], H.C. Shi[71,58], J.L. Shi[12], J.Y. Shi[1], Q.Q. Shi[55], R.S. Shi[1,63], X. Shi[1,58], J.J. Song[20], T.Z. Song[59], W.M. Song[35,1], Y. J. Song[12], Y.X. Song[47,g], S. Sosio[74A,74C], S. Spataro[74A,74C], F. Stieler[36], Y.J. Su[63], G.B. Sun[76], G.X. Sun[1], H. Sun[63], H.K. Sun[1], J.F. Sun[20], K. Sun[61], L. Sun[76], S.S. Sun[1,63], T. Sun[1,63], W.Y. Sun[35], Y. Sun[9], Y.J. Sun[71,58], Y.Z. Sun[1], Z.T. Sun[50], Y.X. Tan[71,58], C.J. Tang[54], G.Y. Tang[1], J. Tang[59], Y.A. Tang[76], L. Y Tao[72], Q.T. Tao[26,h], M. Tat[69], J.X. Teng[71,58], V. Thoren[75], W.H. Tian[52], W.H. Tian[59], Y. Tian[32,63], Z.F. Tian[76], I. Uman[62B], S.J. Wang[50], B. Wang[1], B.L. Wang[63], Bo Wang[71,58], C.W. Wang[43], D.Y. Wang[47,g], F. Wang[72], H.J. Wang[39,j,k], H.P. Wang[1,63], J.P. Wang [50], K. Wang[1,58], L.L. Wang[1], M. Wang[50], Meng Wang[1,63], S. Wang[12,f], S. Wang[39,j,k], T. Wang[12,f], T.J. Wang[44], W. Wang[59], W. Wang[72], W.P. Wang[71,58], X. Wang[47,g], X.F. Wang[39,j,k], X.J. Wang[40], X.L. Wang[12,f], Y. Wang[61], Y.D. Wang[46], Y.F. Wang[1,58,63], Y.H. Wang[48], Y.N. Wang[46], Y.Q. Wang[1], Yaqian Wang[18,1], Yi Wang[61], Z. Wang[1,58], Z.L. Wang[72], Z.Y. Wang[1,63], Ziyi Wang[63], D. Wei[70], D.H. Wei[15], F. Weidner[68], S.P. Wen[1], C.W. Wenzel[4], U.W. Wiedner[4], G. Wilkinson[69], M. Wolke[75], L. Wollenberg[4], C. Wu[40], J.F. Wu[1,63], L.H. Wu[1], L.J. Wu[1,63], X. Wu[12,f], X.H. Wu[35], Y. Wu[71], Y.J. Wu[32], Z. Wu[1,58], L. Xia[71,58], X.M. Xian[40], T. Xiang[47,g], D. Xiao[39,j,k], G.Y. Xiao[43], H. Xiao[12,f], S.Y. Xiao[1], Y. L. Xiao[12,f], Z.J. Xiao[42], C. Xie[43], X.H. Xie[47,g], Y. Xie[50], Y.G. Xie[1,58], Y.H. Xie[6], Z.P. Xie[71,58], T.Y. Xing[1,63], C.F. Xu[1,63], C.J. Xu[59], G.F. Xu[1], H.Y. Xu[66], Q.J. Xu[17], Q.N. Xu[31], W. Xu[1,63], W.L. Xu[66], X.P. Xu[55], Y.C. Xu[78], Z.P. Xu[43], Z.S. Xu[63], F. Yan[12,f], L. Yan[12,f], W.B. Yan[71,58], W.C. Yan[81], X.Q. Yan[1], H.J. Yang[51,e], H.L. Yang[35], H.X. Yang[1], Tao Yang[1], Y. Yang[12,f], Y.F. Yang[44], Y.X. Yang[1,63], Yifan Yang[1,63], Z.W. Yang[39,j,k], Z.P. Yao[50], M. Ye[1,58], M.H. Ye[8], J.H. Yin[1], Z.Y. You[59], B.X. Yu[1,58,63], C.X. Yu[44], G. Yu[1,63], J.S. Yu[26,h], T. Yu[72], X.D. Yu[47,g], C.Z. Yuan[1,63], L. Yuan[2], S.C. Yuan[1], X.Q. Yuan[1], Y. Yuan[1,63], Z.Y. Yuan[59], C.X. Yue[40], A.A. Zafar[73], F.R. Zeng[50], X. Zeng[12,f], Y. Zeng[26,h], Y.J. Zeng[1,63], X.Y. Zhai[35], Y.C. Zhai[50], Y.H. Zhan[59], A.Q. Zhang[1,63], B.L. Zhang[1,63], B.X. Zhang[1], D.H. Zhang[44], G.Y. Zhang[20], H. Zhang[71], H.H. Zhang[59], H.H. Zhang[35], H.Q. Zhang[1,58,63], H.Y. Zhang[1,58], J.J. Zhang[52], J.L. Zhang[21], J.Q. Zhang[42], J.W. Zhang[1,58,63], J.X. Zhang[39,j,k], J.Y. Zhang[1], J.Z. Zhang[1,63], Jianyu Zhang[63], Jiawei Zhang[1,63], L.M. Zhang[61], L.Q. Zhang[59], Lei Zhang[43], P. Zhang[1], Q.Y. Zhang[40,81], Shuihan Zhang[1,63], Shulei Zhang[26,h], X.D. Zhang[46], X.M. Zhang[1], X.Y. Zhang[50], X.Y. Zhang[55], Y. Zhang[69], Y. Zhang[72], Y. T. Zhang[81], Y.H. Zhang[1,58], Yan Zhang[71,58], Yao Zhang[1], Z.H. Zhang[1], Z.L. Zhang[35], Z.Y. Zhang[44], Z.Y. Zhang[76], G. Zhao[1], J. Zhao[40], J.Y. Zhao[1,63], J.Z. Zhao[1,58], Lei Zhao[71,58],

Ling Zhao[1], M.G. Zhao[44], S.J. Zhao[81], Y.B. Zhao[1,58], Y.X. Zhao[32,63], Z.G. Zhao[71,58], A. Zhemchugov[37,a], B. Zheng[72], J.P. Zheng[1,58], W.J. Zheng[1,63], Y.H. Zheng[63], B. Zhong[42], X. Zhong[59], H. Zhou[50], L.P. Zhou[1,63], X. Zhou[76], X.K. Zhou[6], X.R. Zhou[71,58], X.Y. Zhou[40], Y.Z. Zhou[12,f], J. Zhu[44], K. Zhu[1], K.J. Zhu[1,58,63], L. Zhu[35], L.X. Zhu[63], S.H. Zhu[70], S.Q. Zhu[43], T.J. Zhu[12,f], W.J. Zhu[12,f], Y.C. Zhu[71,58], Z.A. Zhu[1,63], J.H. Zou[1], J. Zu[71,58]

[1] *Institute of High Energy Physics, Beijing 100049, People's Republic of China*

[2] *Beihang University, Beijing 100191, People's Republic of China*

[3] *Beijing Institute of Petrochemical Technology, Beijing 102617, People's Republic of China*

[4] *Bochum Ruhr-University, D-44780 Bochum, Germany*

[5] *Carnegie Mellon University, Pittsburgh, Pennsylvania 15213, U.S.A.*

[6] *Central China Normal University, Wuhan 430079, People's Republic of China*

[7] *Central South University, Changsha 410083, People's Republic of China*

[8] *China Center of Advanced Science and Technology, Beijing 100190, People's Republic of China*

[9] *China University of Geosciences, Wuhan 430074, People's Republic of China*

[10] *Chung-Ang University, Seoul, 06974, Republic of Korea*

[11] *COMSATS University Islamabad, Lahore Campus, Defence Road, Off Raiwind Road, 54000 Lahore, Pakistan*

[12] *Fudan University, Shanghai 200433, People's Republic of China*

[13] *G.I. Budker Institute of Nuclear Physics SB RAS (BINP), Novosibirsk 630090, Russia*

[14] *GSI Helmholtzcentre for Heavy Ion Research GmbH, D-64291 Darmstadt, Germany*

[15] *Guangxi Normal University, Guilin 541004, People's Republic of China*

[16] *Guangxi University, Nanning 530004, People's Republic of China*

[17] *Hangzhou Normal University, Hangzhou 310036, People's Republic of China*

[18] *Hebei University, Baoding 071002, People's Republic of China*

[19] *Helmholtz Institute Mainz, Staudinger Weg 18, D-55099 Mainz, Germany*

[20] *Henan Normal University, Xinxiang 453007, People's Republic of China*

[21] *Henan University, Kaifeng 475004, People's Republic of China*

[22] *Henan University of Science and Technology, Luoyang 471003, People's Republic of China*

[23] *Henan University of Technology, Zhengzhou 450001, People's Republic of China*

[24] *Huangshan College, Huangshan 245000, People's Republic of China*

[25] *Hunan Normal University, Changsha 410081, People's Republic of China*

[26] *Hunan University, Changsha 410082, People's Republic of China*

[27] *Indian Institute of Technology Madras, Chennai 600036, India*

[28] *Indiana University, Bloomington, Indiana 47405, U.S.A.*

[29] *INFN Laboratori Nazionali di Frascati, (A)INFN Laboratori Nazionali di Frascati, I-00044, Frascati, Italy; (B)INFN Sezione di Perugia, I-06100, Perugia, Italy; (C)University of Perugia, I-06100, Perugia, Italy*

[30] *INFN Sezione di Ferrara, (A)INFN Sezione di Ferrara, I-44122, Ferrara, Italy; (B)University of Ferrara, I-44122, Ferrara, Italy*

[31] *Inner Mongolia University, Hohhot 010021, People's Republic of China*

[32] *Institute of Modern Physics, Lanzhou 730000, People's Republic of China*

[33] *Institute of Physics and Technology, Peace Avenue 54B, Ulaanbaatar 13330, Mongolia*

[34] *Instituto de Alta Investigación, Universidad de Tarapacá, Casilla 7D, Arica, Chile*

[35] *Jilin University, Changchun 130012, People's Republic of China*

[36] *Johannes Gutenberg University of Mainz, Johann-Joachim-Becher-Weg 45, D-55099 Mainz, Germany*

[37] *Joint Institute for Nuclear Research, 141980 Dubna, Moscow region, Russia*

[38] *Justus-Liebig-Universitaet Giessen, II. Physikalisches Institut, Heinrich-Buff-Ring 16, D-35392 Giessen, Germany*

[39] *Lanzhou University, Lanzhou 730000, People's Republic of China*

[40] *Liaoning Normal University, Dalian 116029, People's Republic of China*

[41] *Liaoning University, Shenyang 110036, People's Republic of China*

[42] *Nanjing Normal University, Nanjing 210023, People's Republic of China*

[43] *Nanjing University, Nanjing 210093, People's Republic of China*

[44] *Nankai University, Tianjin 300071, People's Republic of China*

[45] *National Centre for Nuclear Research, Warsaw 02-093, Poland*

[46] *North China Electric Power University, Beijing 102206, People's Republic of China*

[47] *Peking University, Beijing 100871, People's Republic of China*

[48] *Qufu Normal University, Qufu 273165, People's Republic of China*

[49] *Shandong Normal University, Jinan 250014, People's Republic of China*

[50] *Shandong University, Jinan 250100, People's Republic of China*

[51] *Shanghai Jiao Tong University, Shanghai 200240, People's Republic of China*

[52] *Shanxi Normal University, Linfen 041004, People's Republic of China*

[53] *Shanxi University, Taiyuan 030006, People's Republic of China*

[54] *Sichuan University, Chengdu 610064, People's Republic of China*

[55] *Soochow University, Suzhou 215006, People's Republic of China*

[56] *South China Normal University, Guangzhou 510006, People's Republic of China*

[57] *Southeast University, Nanjing 211100, People's Republic of China*

[58] *State Key Laboratory of Particle Detection and Electronics, Beijing 100049, Hefei 230026, People's Republic of China*

[59] *Sun Yat-Sen University, Guangzhou 510275, People's Republic of China*

[60] *Suranaree University of Technology, University Avenue 111, Nakhon Ratchasima 30000, Thailand*

[61] *Tsinghua University, Beijing 100084, People's Republic of China*

[62] *Turkish Accelerator Center Particle Factory Group, (A)Istinye University, 34010, Istanbul, Turkey; (B)Near East University, Nicosia, North Cyprus, 99138, Mersin 10, Turkey*

[63] *University of Chinese Academy of Sciences, Beijing 100049, People's Republic of China*

[64] *University of Groningen, NL-9747 AA Groningen, The Netherlands*

[65] *University of Hawaii, Honolulu, Hawaii 96822, U.S.A.*

[66] *University of Jinan, Jinan 250022, People's Republic of China*

[67] *University of Manchester, Oxford Road, Manchester, M13 9PL, United Kingdom*

[68] *University of Muenster, Wilhelm-Klemm-Strasse 9, 48149 Muenster, Germany*

[69] *University of Oxford, Keble Road, Oxford OX13RH, United Kingdom*

[70] *University of Science and Technology Liaoning, Anshan 114051, People's Republic of China*

[71] *University of Science and Technology of China, Hefei 230026, People's Republic of China*

[72] *University of South China, Hengyang 421001, People's Republic of China*

[73] *University of the Punjab, Lahore-54590, Pakistan*

[74] *University of Turin and INFN, (A)University of Turin, I-10125, Turin, Italy; (B)University of Eastern Piedmont, I-15121, Alessandria, Italy; (C)INFN, I-10125, Turin, Italy*

[75] *Uppsala University, Box 516, SE-75120 Uppsala, Sweden*

[76] *Wuhan University, Wuhan 430072, People's Republic of China*

[77] *Xinyang Normal University, Xinyang 464000, People's Republic of China*

[78] *Yantai University, Yantai 264005, People's Republic of China*

[79] *Yunnan University, Kunming 650500, People's Republic of China*

[80] *Zhejiang University, Hangzhou 310027, People's Republic of China*

[81] *Zhengzhou University, Zhengzhou 450001, People's Republic of China*

[a] *Also at the Moscow Institute of Physics and Technology, Moscow 141700, Russia*

[b] *Also at the Novosibirsk State University, Novosibirsk, 630090, Russia*

[c] *Also at the NRC "Kurchatov Institute", PNPI, 188300, Gatchina, Russia*

[d] *Also at Goethe University Frankfurt, 60323 Frankfurt am Main, Germany*

[e] *Also at Key Laboratory for Particle Physics, Astrophysics and Cosmology, Ministry of Education; Shanghai Key Laboratory for Particle Physics and Cosmology; Institute of Nuclear and Particle Physics, Shanghai 200240, People's Republic of China*

[f] *Also at Key Laboratory of Nuclear Physics and Ion-beam Application (MOE) and Institute of Modern Physics, Fudan University, Shanghai 200443, People's Republic of China*

^{g} *Also at State Key Laboratory of Nuclear Physics and Technology, Peking University, Beijing 100871, People's Republic of China*

^{h} *Also at School of Physics and Electronics, Hunan University, Changsha 410082, China*

^{i} *Also at Guangdong Provincial Key Laboratory of Nuclear Science, Institute of Quantum Matter, South China Normal University, Guangzhou 510006, China*

^{j} *Also at Frontiers Science Center for Rare Isotopes, Lanzhou University, Lanzhou 730000, People's Republic of China*

^{k} *Also at Lanzhou Center for Theoretical Physics, Lanzhou University, Lanzhou 730000, People's Republic of China*

^{l} *Also at the Department of Mathematical Sciences, IBA, Karachi 75270, Pakistan*